Polycaprolactone-based Block Copolymers. II. Morpholology and Crystallization of Copolymers of Styrene or Butadiene and ϵ-Caprolactone

J. HEUSCHEN,* R. JÉRÔME,† and PH. TEYSSIÉ, *Laboratory of Macromolecular Chemistry and Organic Catalysis, University of Liège, Sart-Tilman B6, B4000 Liege, Belgium*

Synopsis

Three series of amorphous semicrystalline poly(styrene-*b*-ϵ-caprolactone)s have been synthesized with polystyrene blocks of 6000 (series A), 40000 (series B), and 70000 (series C) molecular weight, respectively. In these materials, the polymer miscibility evolves from a situation where a diffuse interphase involves the major part of the volume of the copolymer (series A) to a sharp phase separation as observed for copolymers with the longest PS block (series C). The crystallization of PCL blocks is mainly governed by the phase morphology. In copolymers of series A, the crystallization rate of PCL blocks is slowed down the more as the miscibility with PS increases, and ultimately the degree of crystallinity X_c decreases significantly. When phase separation is sharp, X_c changes dramatically at the phase inversion and decreases when PS forms the continuous phase. At the inversion, X_c depends on the mean size of the PCL microdomains as compared with the thickness of the crystalline lamellae. The periodicity of the phase morphology as observed by TEM is influenced by the solvent used in casting films, whereas monolamellar monocrystals can be obtained by a self-seeding technique.

INTRODUCTION

When they associate immiscible components, block and graft polymers generally display characteristic and very attractive properties. The formation of highly organized structures into mesomorphic phases is well documented,[1] and thermoplastic elastomers based on this type of polymer have reached commercial development.[2] Nowadays, block and graft polymers are receiving much attention as surface-active compounds. These materials find their way as surfactants in water-oil and oil-oil systems.[3,4] In the latter case, the oil phases are either solid and give rise to polymeric alloys[5,6] or liquid and allow the preparation of latexes in organic media.[7] Dispersions of fine solid particles into liquids can also be stabilized by appropriate block or graft copolymers which provide the dispersed particles with an efficient coalescence barrier.[8] When mixed within a polymeric matrix, a few percent of a well-chosen two-phase copolymer can diffuse to the solid/air interface and profoundly modify the surface properties.[9] This ability to control wettability and adhe-

*Present address: General Electric Company, Technology Department, Mt. Vernon, Mt. Vernon, Indiana 47620.
†To whom correspondence should be addressed.

Journal of Polymer Science: Part B: Polymer Physics, Vol. 27, 523–544 (1989)

CCC 0098-1273/89/030523-22$04.00

sive or frictional properties of commodity or engineering commercial resins deserve great interest for new technological applications.

From this rapid survey of the opportunities offered by block and graft polymers, it is obvious that their remarkable behavior results from their unique capability of combining the useful properties of the associated macromolecular species. Thus, poly(ϵ-caprolactone) (PCL) occupies a favorable position, owing to its low-temperature adhesiveness,[10] its ability to disperse pigments,[10] and its miscibility with various commercial polymers, including poly(vinyl chloride) (PVC), poly(styrene-co-acrylonitrile), ABS resins, nitrocellulose, cellulose propionate and butyrate, poly(epichlorohydrin), and bisphenol A polycarbonate.[10,11] Furthermore, PCL is biodegradable, and its lack of toxicity makes this polyester a candidate for applications in the rapidly growing field of controlled-release drugs.[10-12] Undoubtedly, copolymers containing PCL blocks also might contribute to the control of surface properties, e.g., adhesiveness and printability. They are good interfacial agents in polymer blends comprising all the polymers miscible with PCL for which the availability of related block polymers is quite a problem.[13] Blends of PCL and any other biocompatible polymers could also be instrumental in the design of new biomaterials and drug delivery systems.

A few years ago, a new family of bimetallic μ-oxoalkoxides was developed as very active anionic-coordinate-type catalysts in the living polymerization of ϵ-caprolactone (ϵ-CL).[14] The knowledge of the structural and kinetic behavior of these oxoalkoxides has opened the way to original polymer (PX)-supported catalysts that are powerful in tailoring PCL block polymers with well-controlled molecular parameters.[15] Poly(styrene-*b*-ϵ-caprolactone) copolymers (PS-PCL) have been synthesized and their mesomorphic organization discussed elsewhere.[16-18] Briefly, these copolymers display liquid-crystalline structures at room temperature and in the presence of a selective solvent of the amorphous PS block. When the composition ranges from 40 to 65 wt% of PCL, a lamellar crystalline structure is obtained in the presence of diethylphthalate. The lamellar structure and especially the number of folds and crystallinity of the PCL block have been investigated in relation to both the copolymer composition and the solvent concentration.

Considering the possible application to PX-PCL diblock polymers as interfacial agents, especially in immiscible polymer blends (PX blended with PCL or any polymer miscible with PCL), it is of prime interest to know how the immiscibility of PX and PCL blocks changes with molecular weight as well as the effect of block polymerization on the crystallization of PCL in the absence of any solvent. In order to answer these questions, three series of PS-PCL diblock polymers have been synthesized based on PS of 6,000, 40,000, and 70,000 molecular weight, respectively (Table I). A poly(butadiene-*b*-ϵ-caprolactone) (PBD-PCL) sample has also been used in order to evaluate to which extent the softness of the associated PX block can affect the behavior of the polyester block.

EXPERIMENTAL

Di-μ-oxo-bis[bis(1-methylethoxy)aluminum]zinc was the initial catalyst, the isopropyloxy groups of which were replaced by 2-ethylhexanoate and

TABLE I
Molecular Weight and Weight Composition of PCL-containing Diblock Copolymers

Sample	$\bar{M}_n$ copolymer	$\bar{M}_n$ PSt	$\bar{M}_n$ PCL	Wt% PCL	Wt% PSt
A1	9,600	6,000	3,800	37	63
A2	12,000	6,000	6,000	50	50
A3	14,500	6,000	8,500	59	41
A4	16,000	6,000	10,000	62	38
A5	18,000	6,000	12,000	67	33
B1	45,000	40,000	5,000	11	89
B2	54,000	40,000	14,000	26	74
B3	78,000	40,000	38,000	49	51
B4	87,000	40,000	47,000	54	46
B5	140,000	40,000	100,000	70	30
C1	105,000	70,000	35,000	33	67
C2	125,000	70,000	55,000	44	56
C3	160,000	70,000	90,000	56	44
Sample	$\bar{M}_n$ copolymer	$\bar{M}_n$ PBD	$\bar{M}_n$ PCL	Wt% PCL	Wt% PBD
F1	45,000	15,000	30,000	66	34

hydroxy-terminated PX (PS or PBD), respectively. The living block polymerization of ϵ-CL proceeded through the selective acyl-oxygen cleavage of the lactone with insertion into the Al-OPX bond of the polymer-supported catalyst, all the Al-2-ethylhexanoate bonds being practically inactive. Copolymerizations were carried out under an argon atmosphere in a previously dried glass reactor. Synthesis of the catalyst, copolymerization procedure, and characterization of copolymers are extensively described elsewhere.[15]

The morphology of the solvent-cast films was examined by transmission electron microscopy in a JEOL Model JEM 100 U microscope and by optical microscopy under polarized light.

The thermal properties of all samples were measured by using a Du Pont 990 thermal analyzer. A Gehman torsion pendulum was used to record isochronal (10 s) curves of torsion modulus versus temperature.

RESULTS AND DISCUSSION

Multiphase Character of the PS-PCL and PBD-PCL Copolymers

When the question of immiscibility of polymers is addressed, it is usual to measure the glass transition temperature(s) of the multicomponent system.[11] Provided their molecular weights are high enough, PS-PCL block polymers can be molded into samples well suited to record isochronous torsion modulus-temperature curves. Figure 1 shows the thermal dependence of the torsion modulus as measured 10 s after the deformation for the series of block polymers based on PS of the higher molecular weight (70 K); curves relative to comparable homopolymers are also recorded for comparison. The main information derived from these mechanical measurements is summarized in Table II. Although the degree of crystallinity (X_c) of PCL is rather high

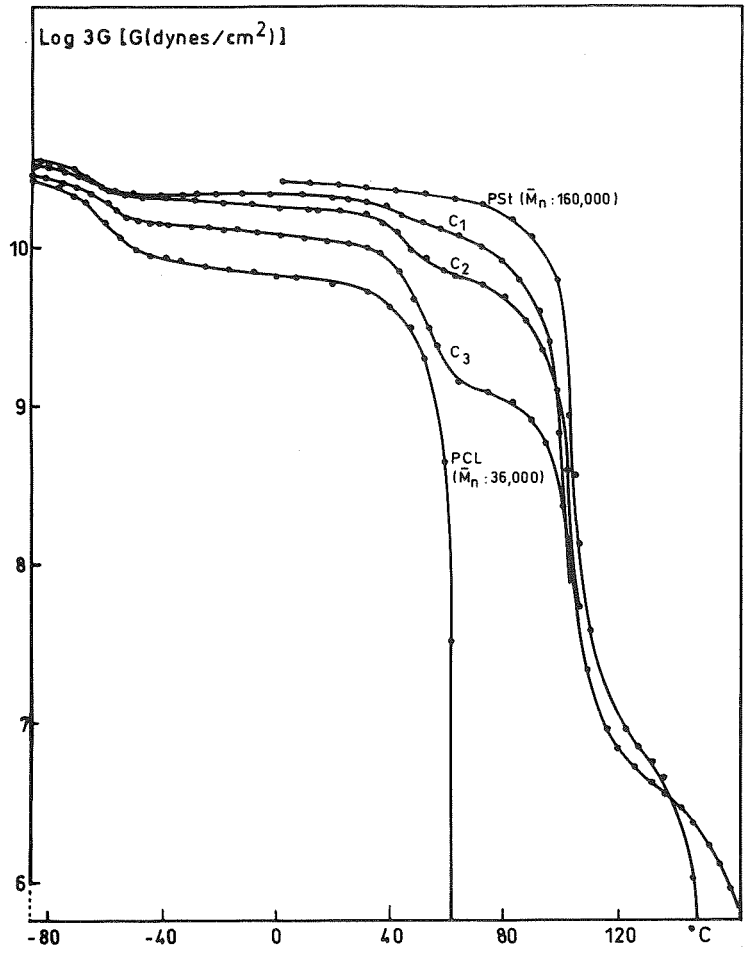

Fig. 1. Thermal dependence of the isochronous (10 s) torsion modulus for poly(styrene-*b*-ϵ-caprolactone)s of series C (see Table I).

TABLE II
Glass Transition Temperature (T_g) and Melting Temperature (T_m) for Poly(styrene-*b*-ϵ-caprolactone)s as Determined from Isochronous Torsion Modulus-Temperature Curves

Sample	Composition (wt%) PSt	Composition (wt%) PCL	T_g PCL (°C)	T_m PCL (°C)	T_g PSt (°C)
C1	67	33	−65	43	98
C2	56	44	−62	45	100
C3	44	56	−60	50	100
Homo PSt ($\bar{M}_n$ = 160,000)			—	—	101
Homo PCL ($\bar{M}_n$ = 36,000)			−60	59	—

(50–60%),[19] the glass transition temperature (T_g) of the minor amorphous phase is unambiguously detected. This is also true for copolymers where T_g of PCL decreases regularly from −60 to −65°C when the percentage of PCL goes down. Since T_g of PCL is known to decrease with X_c (−60°C for X_c = 50%, and −71°C for X_c = 0),[20,21] it might be anticipated that PCL blocks crystallize less as their percentage in the copolymer decreases. This behavior is experimentally confirmed and discussed below. Melting of PCL is responsible for a drop of the torsion modulus, the sharper as the PCL percentage increases. The melting temperature recorded at the half-height of the corresponding modulus drop decreases substantially, whereas the temperature range of melting broadens when the percentage of PS increases. These features are indicators of morphological effects on the crystallization of the PCL blocks as discussed afterwards.

The poor mechanical strength of both the PS-PCL copolymers of series A and B and the PBD-PCL sample has prevented any reliable measurements of the torsion modulus. Although it is less sensitive for detecting T_g of semicrystalline polymers, differential thermal analysis (DSC) has been used to determine the main transitions in the lower molecular weight PS–PCL and in PBD-PCL copolymers. Figure 2 illustrates the DSC isothermal crystallization at 44°C for 1 h. When PS is the major component (B1 and B2), the T_g of PS is observed at about 95°C, whereas the poor sensitivity of DSC is more likely to prevent the observation of T_g of PCL (or PCL-rich) phases. Furthermore, these phases provide no evidence of significant crystallinity as supported by the absence of a melting endotherm. For samples containing at least 50 wt% of PCL, the T_g of this component becomes visible as well as its melting endotherm which extends over the temperature range where the T_g of PS should be observed.

PS-PCL copolymers of series A display thermal behavior significantly different from that of series B. Figure 3 shows the thermogram of the copolymers recovered by precipitation into a cyclohexane/hexane nonsolvent mixture (curve a). Even at a percentage smaller than 50 wt%, PCL blocks are crystalline and exhibit a well-defined melting temperature, while the observation of the glass transition is quite puzzling. This drawback can be alleviated by very fast cooling of the melted polymers maintained 5 min at 130°C. The quenching of sample Al completely prevents the short PCL block from crystallizing and allows a unique but very broad T_g to be observed at a temperature intermediate between T_g of the corresponding homopolymers (−71 and +78°C; Fig. 3, trace b). It is worth stressing that these homopolymers are immiscible as supported by the macrophase separation in a solvent-cast film of the related blend. The apparent miscibility of the PS (6000) and PCL (3600) blocks is therefore the consequence of the covalent bond linking these two polymers to each other. When its chain length increases, the PCL block crystallizes upon heating the quenched sample (curves b, Fig. 3). For copolymers A2 and A3, the crystallization exotherm starts at about 10°C, and a still broad T_g is reported (Table III). Thermograms of copolymers A4 and A5 are completely dominated by the succession of crystallization and melting events, so that no glass transition can be observed. T_g values reported for the quenched samples are clues to the miscibility of the short length PS and PCL blocks. Nevertheless, the breadth of the glass transition means that only

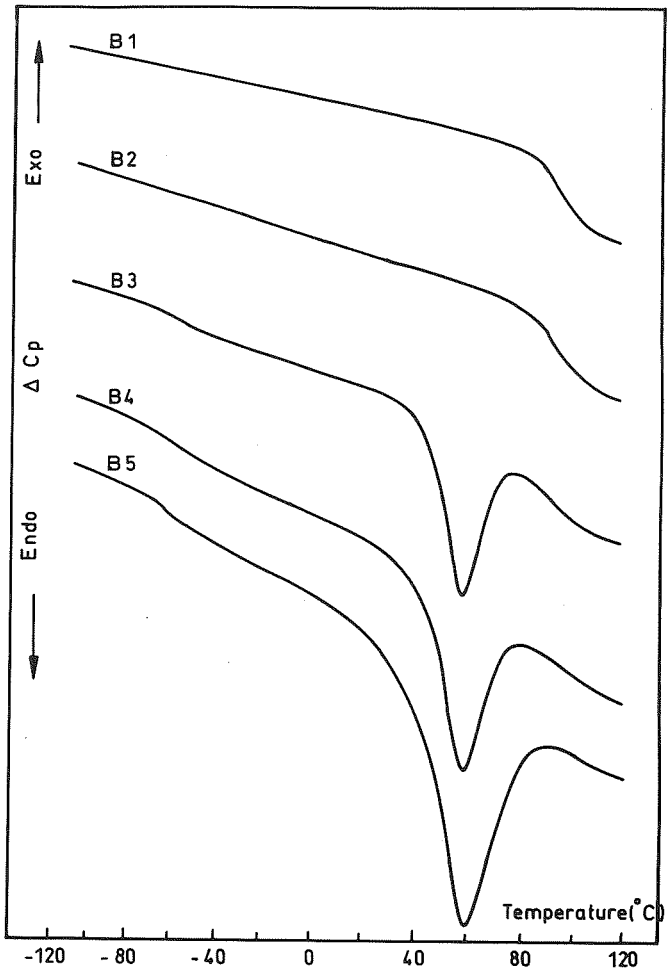

Fig. 2. Differential thermal analysis of poly(styrene-*b*-ϵ-caprolactone)s of series B (see Table I) crystallized at 44°C for 1 h. Heating rate: 20°C/min.

partial miscibility occurs in the molten state, and that speaking of a more or less extended diffuse interface should be more appropriate.

In conclusion, the three series of amorphous-semicrystalline PS-PCL copolymers reported in Table I cover a very large range of miscibility while going from materials where the diffuse interphase extends to most of the volume of the sample (Al) to copolymers of high molecular weight characterized by a very thin diffuse phase boundary as assessed by two T_g's very close to those of the related homopolymers (series C). Composition of the copolymers is another key parameter in controlling crystallization of the PCL blocks. This phenomenon occurs as soon as PCL is no longer the minor component. However, it can be observed earlier when the chain length of PS is short enough (6000), i.e., in a copolymer containing only 37 wt% of PCL (Al).

That the PBD-PCL copolymer (Table I) is microphase separated is convincingly illustrated by the thermogram of Figure 4, where T_g of polybutadiene is expectedly observed at -87°C, and the melting of PCL occurs at 60°C.

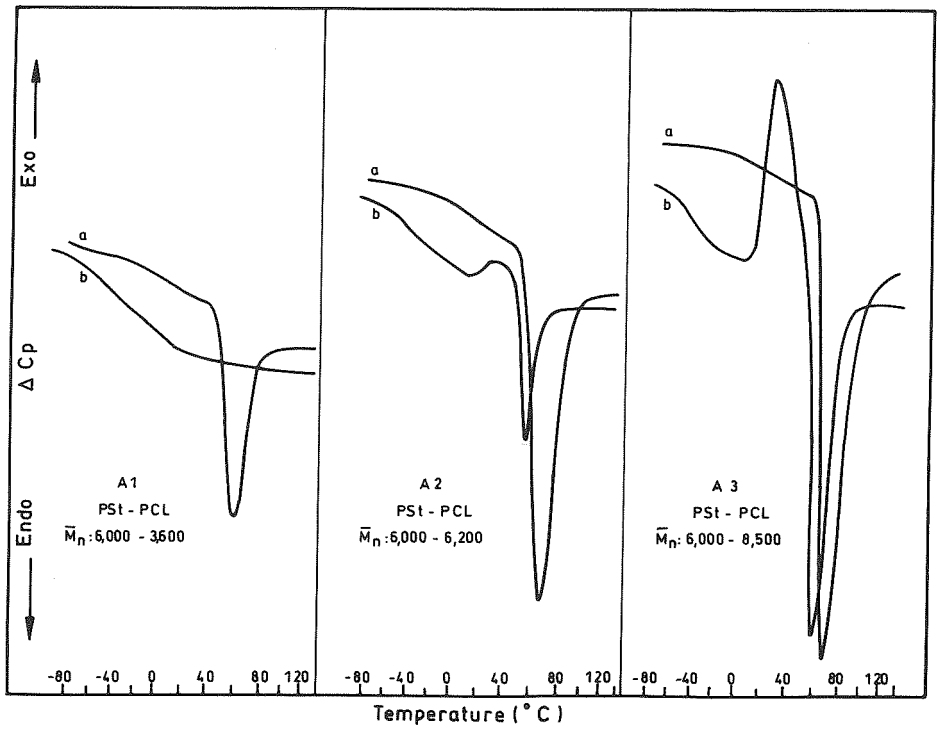

Fig. 3. Differential thermal analysis of poly(styrene-*b*-ϵ-caprolactone)s of series A (see Table I) as recovered by precipitation (trace a) and quenched from the melt (trace b). Heating rate: 20°C/min.

Although the main thermal transition exhibited by PS-PCL polymers of series B and C unambiguously conclude to their multiphase character, this structural feature would be advantageously visualized by the direct observation of the phase morphology.

Very thin films (about 500 Å) have been cast from highly dilute copolymer solution (0.1 %) in benzene which is a good solvent of each block. Indeed, the exponent a of the Mark–Houwink viscometric relation ($[\eta] = K \cdot M^a$) is 0.74 and 0.73 for PS and PBD, respectively, at 25°C,[22] and 0.82 for PCL at 30°C.[23] Transmission electron microscopy fails to detect any well-defined microphase structure in thin films of copolymers of series A, which is in quite good agreement with the results of thermal analysis. In contrast, copolymers of series B and C show a sharp microphase separation, indicating that the

TABLE III
Glass Transition Temperature Range as Observed for Quenched Poly(styrene-*b*-ϵ-caprolactone)s of Series A

Sample	T_g range (°C)	Average T_g (°C)
A1	−53 to +20	−15
A2	−60 to +10	−25
A3	−60 to +32	−46

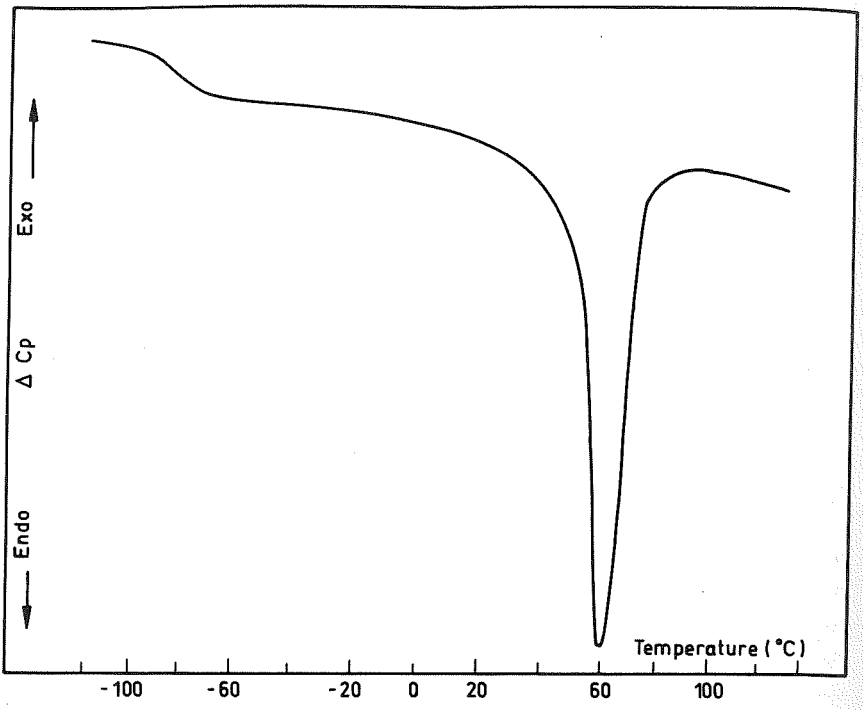

Fig. 4. Differential thermal analysis of poly(butadiene-*b*-ϵ-caprolactone) (see Table I). Heating rate: 20°C/min.

difference in electron density of PS and PCL is great enough to allow multiphase morphology to be observed. From the electron micrographs of copolymers C1, C2, and C3 (Fig. 5), the darkest phases may be attributed to PCL and the lightest to PS. Indeed, PCL, which is the minor component in copolymer C1 has to form the dispersed phases. The situation has been reversed in copolymer C2 containing 44 wt% PCL. Accordingly the phase inversion should occur between 33 and 44 wt% PCL. In series B, microphase structures are of the same type as those observed for series C, except for copolymer B3 which displays a local lamellar organization (Fig. 6). It is well known that a lamellar periodic morphology is characteristic of copolymer with composition near 50 : 50. However, when a semicrystalline/amorphous polymer is considered, the nascent crystallization of one block might induce locally a preferential radial orientation of the phases. Table IV summarizes the mean size of the microdomains that expectedly increases with the chain length of the blocks. Figure 7 shows the phase morphology of the PBD-PCL copolymer, the PBD block of which has been previously stained by osmium tetroxide. Roughly spherical domains of PBD are observed with a mean size of 500 Å, i.e., significantly bigger than sizes reported for comparable PS-PCL copolymers (B2). This conclusion may be explained by a higher degree of immiscibility of the PBD/PCL pair compared with that of the PS/PCL pair. This experimental observation is in a qualitative agreement with values of the solubility parameter (S) for each block, i.e., 8.4, 9.1, and 10.2 $(cal/cm^3)^{1/2}$ for PBD, PS, and PCL, respectively.[22] Since the larger the difference in the

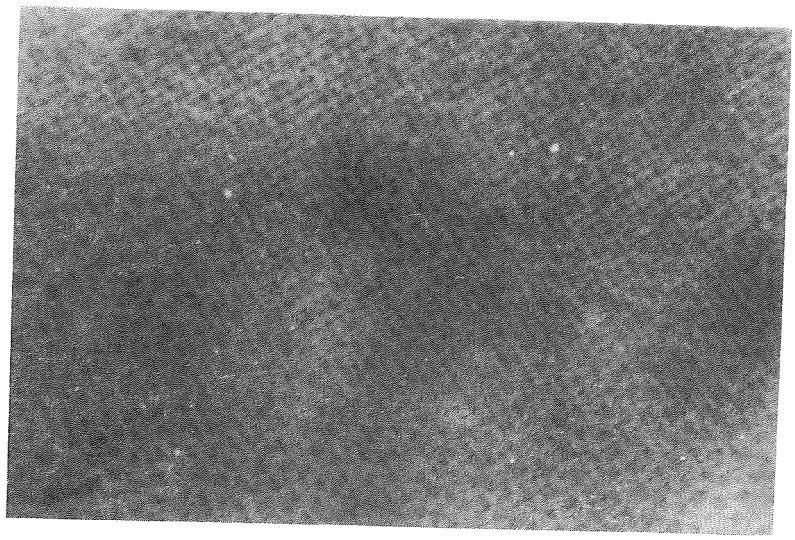

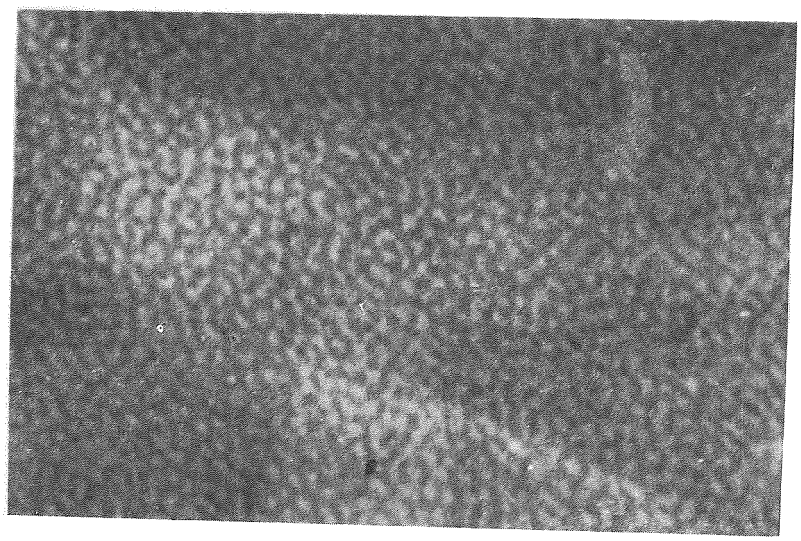

Fig. 5. Transmission electron microscopy of benzene-cast films of poly(styrene-*b*-ϵ-caprolactone)s C1, C2, and C3 (see Table I). The average size of the microdomains is 380 Å (C1), 400 Å (C2) and 500 Å (C3), respectively.

solubility parameter of the associated polymer the higher the degree of immiscibility,[11] it ensues that PBD must be less miscible with PCL than is PS. Finally, the formation of some fibrillar structures may be suspected in Figure 7 and will be substantiated in the next section.

Since the multiphase character of the PBD-PCL and the series of PS-PCL copolymers is now well founded, especially in relation to the composition and molecular weight of PS-containing diblocks, the question is how does crystallization proceed in microphase-separated structures with PCL microdomains

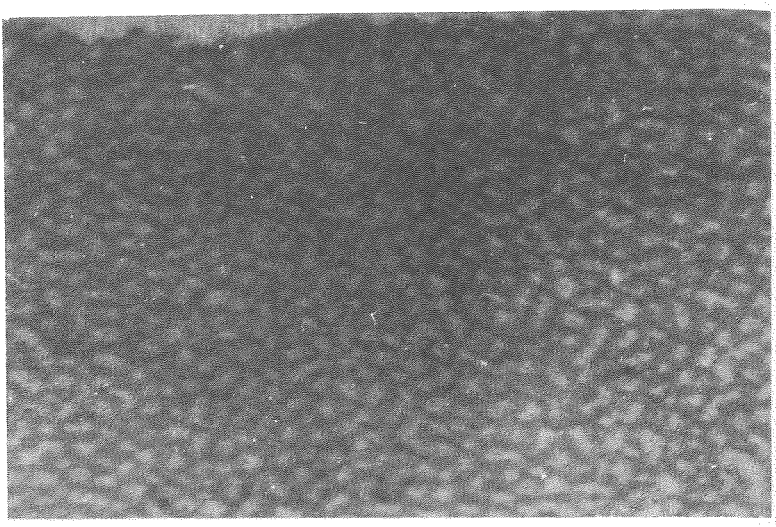

Fig. 5. *(Continued from the previous page.)*

smaller than 500 Å as well as in situations where PCL and PS are semimiscible? Whether the softness or the rigidity of the polymer associated with PCL can influence crystallization is a second question to be addressed.

Crystallization of the PCL Blocks

In order to collect preliminary information on the effect of two-phase morphology on the course of the PCL crystallization, films approximately

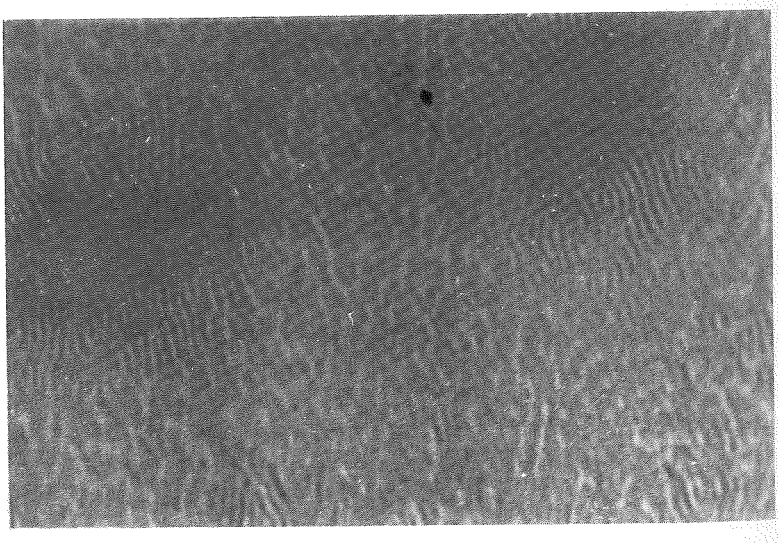

Fig. 6. Transmission electron microscopy of a benzene-cast film of poly(styrene-*b*-ε-caprolactone) B3 (see Table I). The average size of the microdomains is 220 Å.

TABLE IV
Mean Size (d) of the Microdomains Observed in Poly(styrene-*b*-ϵ-caprolactone)s by Transmission Electron Microscopy

Sample	B2	B3	B4	B5	C1	C2	C3
d (Å)	140	220	260	300	380	400	500
$\overline{M}_n$ PSt	40,000	40,000	40,000	40,000	70,000	70,000	70,000
$\overline{M}_n$ PCL	14,000	38,000	47,000	100,000	35,000	55,000	90,000

1 μm thick were observed by optical microscopy under polarized light. They were cast from benzene solution (1 wt%) on a glass plate, melted at 130°C, and then allowed to crystallize at 40°C. Figure 8 compares optical micrographs of PCL and block copolymers (series B) of decreasing PCL content. Spherulites of comparable size are formed, but the quality of the crystalline texture is perturbed the more deeply as the PS content increases. When PS forms the continuous phase, no crystalline structure is evidenced. It must be remembered that the electron microscopic observation of these samples has shown the presence of dispersed PCL domains of about 0.04 μm, which is much smaller than the resolution of optical microscopy (about 1 μm). Turning again to the PCL-rich copolymers, the dispersed PS component is below T_g at the crystallization temperature (40°C) and counteracts the radial growth of crystalline fibrils into spherulites. The situation should therefore be much more favorable when PS is substituted by a rubbery component, like PBD. This prediction is completely supported by Figure 9A relative to the PBD-PCL copolymer, since the spherulitic texture is now very similar to that of the homopolyester. As reported in the preceding section (Fig. 7), the electron micrograph of a thin benzene-cast film of PBD-PCL shows crystalline fibrils belonging to growing spherulites. Another area of the same sample observed at

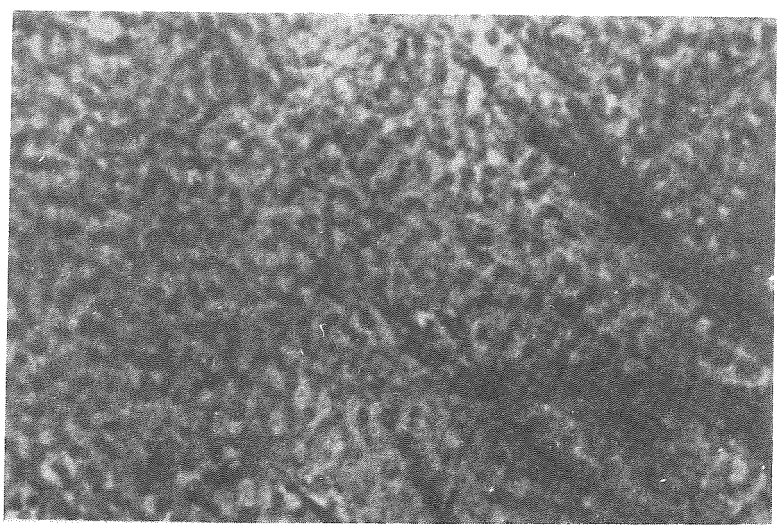

Fig. 7. Transmission electron microscopy of a benzene-cast film of poly(butadiene-*b*-ϵ-caprolactone) (see Table I). The average size of the microdomains is 500 Å.

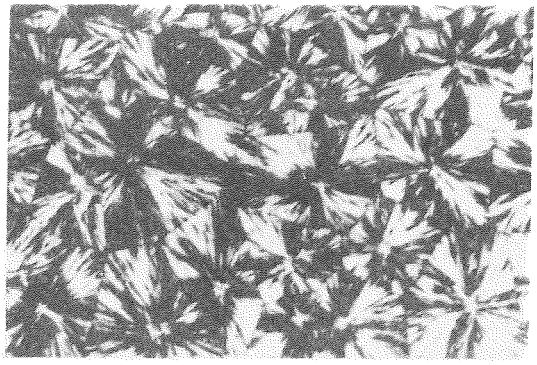

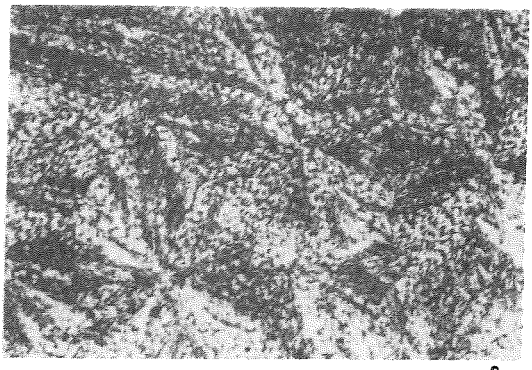

Fig. 8. Optical microscopy of poly(ϵ-caprolactone) and poly(styrene-*b*-ϵ-caprolactone)s of series B (see Table I) (G = 260).

a lower magnification (Fig. 10) illustrates the unperturbed growth of a PCL spherulite (about 15 μm). The soft PBD component does not prevent that spherulite formation, but it is very instrumental in emphasizing its contour length. Indeed, the easily deformed PBD domains concentrate at the periphery of the crystalline fibrils and makes the observation very easy in contrast to spherulite growth in the homopolyester. Finally, the crystalline behavior of copolymers of series A is different and characterized by the formation of smaller spherulites weakly affected by the PS component (Fig. 9B). This is consistent with a crystallization process occurring in a nearly homogeneous melted phase, whereas a two-phase melted system must prevail at 40°C in copolymers of series B and C

Although optical and electron micrographs have already shed light on the effect that block polymerization can have on crystallization of PCL, much more quantitative information should result from measurements of melting temperature (T_m), degree of crystallinity (X_c), and crystallization rate as approximated by the half-crystallization time ($t_{1/2}$) of PCL blocks. Data relative to copolymers of series A are collected in Table V in comparison to homopolyesters of the same chain length as the PCL blocks. All the samples have been crystallized at a constant temperature of 44°C. With the exception

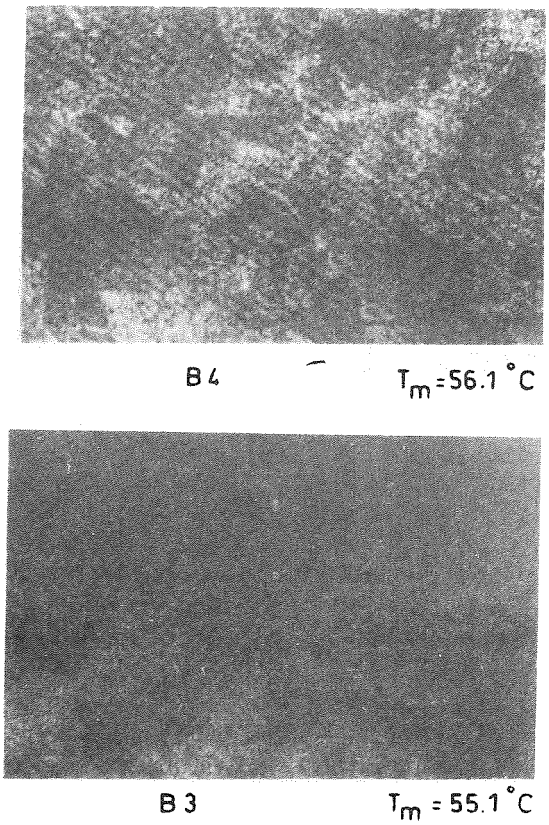

Fig. 8. (*Continued from the previous page.*)

of sample A1, block polymerizing PCL with PS ($\overline{M}_n$ = 6000) has no meaningful effect on T_m, whereas X_c decreases by only 3 or 4%. A dramatic effect is found, however, in the crystallization rate of PCL, which is much slower for block polymers in contrast to homopolymers. Figure 11 illustrates that the slowing down is the more pronounced as the PCL content decreases. This behavior can be accounted for by two arguments. First, previous measurements of T_g have shown an increasing degree of miscibility of PS ($\overline{M}_n$ = 6000) and PCL with decreasing chain length of the latter. Accordingly, while going from copolymers A5 to A1, PCL blocks are increasingly mixed within PS and have to diffuse from that matrix to crystallize into separate domains. Secondly, decreasing the PCL chain length causes the PS percentage and, therefore, T_g of the PS-PCL mixed phase to increase (Table III). It ensues that the gap between that T_g and the crystallization temperature decreases, which expectedly promotes a decrease of the crystallization rate. The very pronounced miscibility of PCL and PS blocks of copolymer A1 also explains why X_c is somewhat depressed, although T_m, i.e., the perfection of the spherulites, is only slightly affected. The general behavior of copolymers of series A is actually comparable to that of the miscible PCL/PVC blends. Several research teams have paid attention to these binary blends and have concluded to the strong dependence of the PCL crystallization on the blend composition.

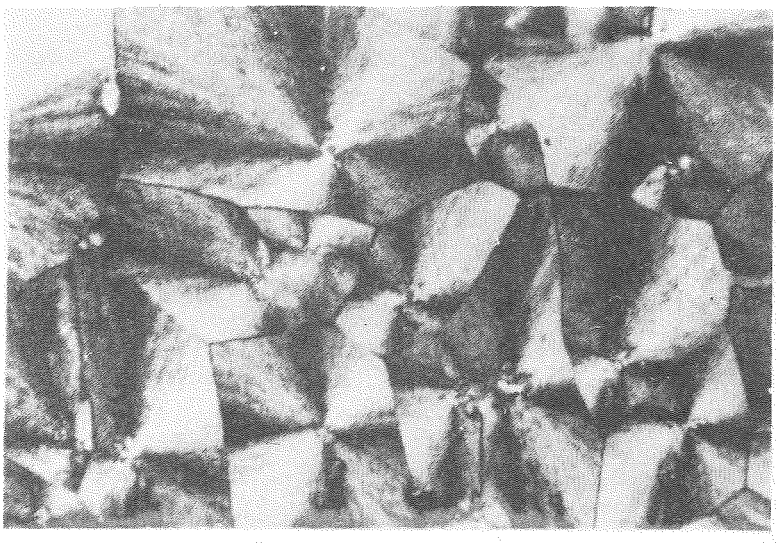

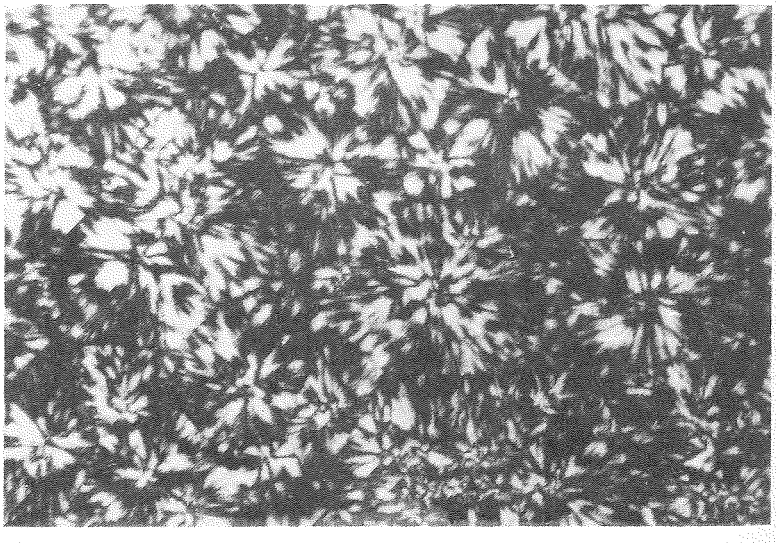

Fig. 9. Optical microscopy of poly(butadiene-*b*-ϵ-caprolactone) F1 and poly(styrene-*b*-ϵ-caprolactone) A4 (see Table I). ($G = 260$).

TABLE V
Melting Temperature (T_m), Degree of Crystallinity (X_c), and Half-crystallization Time ($t_{1/2}$) of PCL Blocks in Poly(styrene-*b*-ϵ-caprolactone) of Series A Compared with the Related Homopolymers

Samples	$t_{1/2}$ (s)	X_c[a] (%)	T_m[a] (°C)
A1	> 9,000[b]	32 ; 43[c]	53
PCL ($\overline{M}_n$ = 3,600)	300	62	56
A2	1,200	54	58
PCL ($\overline{M}_n$ = 6,000)	50	58	58
A4	210	53	59
PCL ($\overline{M}_n$ = 12,000)	65	57	60
A5	160	54	58
PCL ($\overline{M}_n$ = 12,000)	65	57	60

Note: Crystallization temperature = 44°C.
[a]As measured after 18 h.
[b]Upper limit of the DSC apparatus.
[c]As measured after 40 h.

The crystallization rate slows down as the PVC content increases,[24] whereas X_c decreases sharply beyond 60 wt% of PVC.[25]

Figure 11 shows that the crystallization rate of the PCL blocks of series A tends to that of the related homopolyester when the chain length increases, i.e., when the thickness of the diffuse interface decreases. Since copolymers of series B and C exhibit a sharp immiscibility of the two blocks, only T_m and X_c have been systematically measured. Table VI summarizes the experimental data for series B. Once again, block polymerization of PCL does not affect T_m, whereas X_c is strongly dependent on the copolymer composition, as supported by Figure 12. It is obvious that X_c decreases dramatically when the PCL

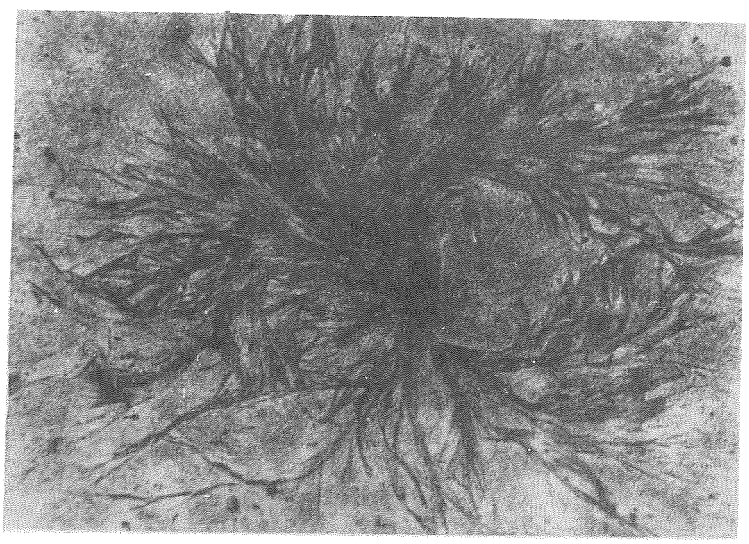

Fig. 10. Transmission electron microscopy of a benzene-cast film of poly(butadiene-*b*-ϵ-caprolactone) F1. The mean size of the spherulites is 15 μm.

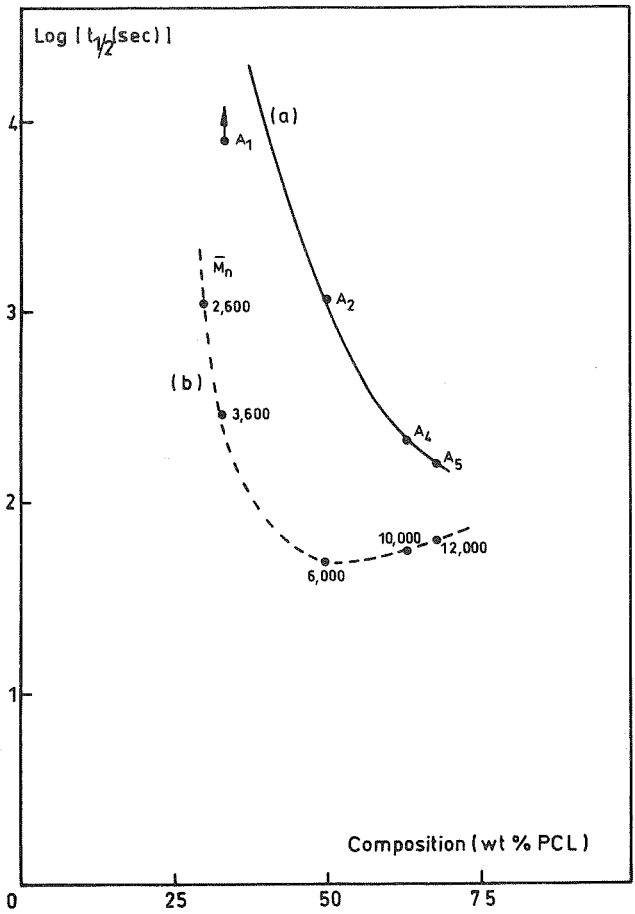

Fig. 11. Half-crystallization time of poly(ε-caprolactone) at 44°C; comparison of polyest block (block copolymers of series A) (curve a) and homopolyester of the same molecular weig (curve b).

TABLE VI
Melting Temperature (T_m) and Degree of Crystallinity (X_c) of PCL Blocks in Poly(styrene-*b*-ε-caprolactone)s of Series B

					Related polyester	
Samples	$\overline{M}_n$ copolymer	% PCL	T_m (°C)	X_c[a] (%)	T_m (°C)	X_c[a] (%
B1	45,000	11	—	0	58	58
B2	54,000	24	55[b]	0	61	55
B3	78,000	49	58	32	61	49
B4	87,000	54	59	36	60	48
B5	140,000	70	60	40	60	44

[a] Crystallization at 44°C for 1 h.
[b] Crystallization at room temperature for several days (X_c = 8%).

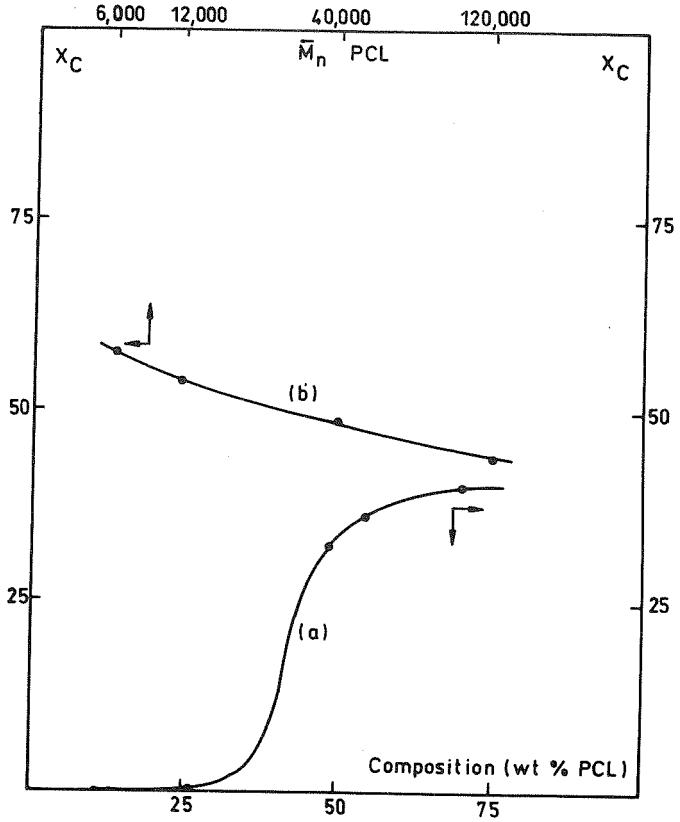

Fig. 12. Degree of crystallinity of poly(ϵ-caprolactone); comparison of polyester block (block copolymers of series B) (curve a) and related homopolyester (curve b).

content decreases below 40 or 45 wt%: it must be remembered that electron microscopy has located the phase inversion in that composition range. Therefore, when PCL forms dispersed phases, its crystallization at 44°C is significantly prevented for 1 h. According to Table IV, the mean size of PCL domains in copolymer B2 is near 140 Å. In these very small phases, constraints are strong enough to impede, or at least to counteract, the crystallization process. This is supported by the very low crystallinity that copolymer B2 displays after 1 week of crystallization at 25°C: X_c is about 8%, and T_m is 6°C lower than the value reported for the related homopolyester. When the other extreme situation is considered, i.e., when PCL is the major component, both X_c and T_m are unaffected by the presence of the PS block.

Since block polymerization perturbs X_c and T_m remains unaffected, Table VII compares the degree of crystallinity of homoPCL and PCL blocks of comparable molecular weight. As previously stressed, when the PCL content of block copolymers decreases, X_c decreases too and especially beyond the phase inversion. In that respect, it is interesting to compare copolymers B2 and C1 which comprise PCL as the dispersed component (about 30 wt% PCL). No crystallinity is observed (1 h at 40°C) in copolymer B2, whereas X_c amounts to 27% when the PCL molecular weight is increased from 14,000 (B2) to 35,000 (C1). This very significant difference is more likely to be related to

TABLE VII
Degree of Crystallinity (X_c) of PCL Block and Polyester of Comparable Molecular Weight

Samples	$\overline{M}_n$ PCL	$\overline{M}_n$ PSt	% PCL	X_c[a] (%)
PCL ($\overline{M}_n$ = 6,000)	6,000	—	100	61
A2	6,000	6,000	50	54
B1	5,000	40,000	11	0
PCL ($\overline{M}_n$ = 12,000)	12,000	—	100	58
A5	12,000	6,000	67	55
B2	14,000	40,000	26	0
PCL ($\overline{M}_n$ = 36,000)	36,000	—	100	55
B3	38,000	40,000	49	31
C1	35,000	70,000	33	27
PCL ($\overline{M}_n$ = 50,000)	50,000	—	100	52
B4	47,000	40,000	54	38
C2	55,000	70,000	44	34
PCL ($\overline{M}_n$ = 120,000)	120,000	—	100	50
B5	100,000	40,000	70	49
C3	90,000	70,000	56	40

[a] Crystallization at 40°C for 1 h.

the mean size of the PCL phases, which has been estimated to be 140 Å for B2 and 380 Å for C1 (Table IV). Since PCL of comparable chain length forms crystalline lamellae with a thickness of about 150 Å,[19] crystallization is expected to be dramatically hindered in copolymer B2, in contrast to C1. Nevertheless, PCL blocks are still constrained in the small domains of C1, accounting for a decrease in T_m by 8°C compared with the corresponding homopolyester. When the PCL content is at least 50 wt%, X_c is higher for the shorter PCL block (copolymers A1, B4, and C3 in Table VII), and this is qualitatively consistent with the general behavior of the homopolymer itself.

Finally, the PBD-PCL block polymer exhibits practically the same crystalline features as the related polyester, i.e., the same X_c (55%) and a slightly lower T_m (58°C instead of 61°C).

Organization of the Two-phase Morphology of PS-PCL Block Polymers

Transmission electron micrographs have convincingly demonstrated the two-phase character of the PS–PCL diblock polymers. Nevertheless, in contrast to amorphous-amorphous diblocks, such as poly(styrene-*b*-butadiene),[1,26] no periodic structure (lamellar structure, hexagonal lattice, face-centered cubic lattice) has been observed. Of course, it is well-known that the phase morphology of completely amorphous block polymers is strongly dependent on the conditions used in producing the sample.[27] Most often a solvent is used for its selectivity toward one of the two blocks. Furthermore, the evaporation rate and any further thermal treatment may have a pronounced effect on the ultimate phase structure. When one component of block polymers is semicrystalline, organizing the phase morphology is still more difficult because the crystallization process can either perturb a well-organized two-phase structure

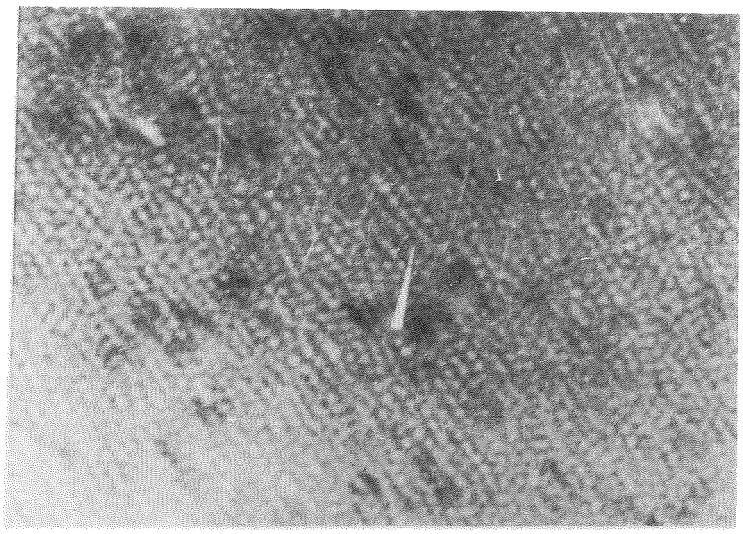

Fig. 13. Transmission electron microscopy of a cyclohexane-cast film of poly(styrene-*b*-ϵ-caprolactone) B2 (see Table I).

or freeze-in a not yet organized phase morphology. From these considerations, films of PS-PCL copolymers should be cast from a selective solvent of PS or PCL, rather than from benezene. A selective solvent of PS has thus been selected in order to favor the crystallization of the insoluble PCL blocks; in that way, micelles comprising a crystallized PCL core should be formed with an approximately constant size and maintained in solution by the soluble PS blocks. This approach has been carried out using a block polymer with a minor PCL component (B2) and cyclohexane as a selective solvent of PS. Actually, the block polymer is dissolved at 65°C at a concentration of 0.1 wt%. During subsequent cooling and solvent evaporation, the expected micelles form, whereas PS tends to build up a matrix embedding the crystalline microdomains of PCL. Figure 13 shows that the periodicity of the phase morphology has been significantly improved in comparison with that previously observed for benzene-cast films. Although there is a visible trend for a hexagonal lattice to be formed, the quality of the organization is not yet comparable to that of the completely amorphous block polymers. During the ultimate step of solvent evaporation, the crystalline component (dark phase) does not remain dispersed but seems to condense into a minor continuous phase. Although effort was devoted to the improvement of this preliminary but encouraging result, attention has also been paid to precipitation, and therefore crystallization, of the PCL blocks in a selective solvent of PS blocks.

It is well-known that some homopolymers can be precipitated from dilute solutions with formation of monocrystals; among others, poly(ethylene oxide) and polyethylene have been extensively investigated.[28-30] Although this is less well documented in the scientific literature, some amorphous-crystalline block polymers have been successfully recovered as monocrystals,[31-35] and the contribution of Lotz, Kovacs and collaborators dealing with poly(styrene-*b*-ethylene oxide) are of great interest.[33] The possible formation of monocrystals

of PS-PCL block polymers has been considered, and, after a preliminary investigation, isoamyl acetate has been selected as a suitable selective nonsolvent of PCL blocks. Furthermore, formation of monocrystals in isoamyl acetate is easily observed because the refractive indices of the two components are different. Taking advantage of the self-seeding technique,[36] monolamellar monocrystals of copolymer B4 (54 wt% PCL) have been obtained (Fig. 14): they are approximately 10 μm long and 2.5 μm wide. Features of the electron-

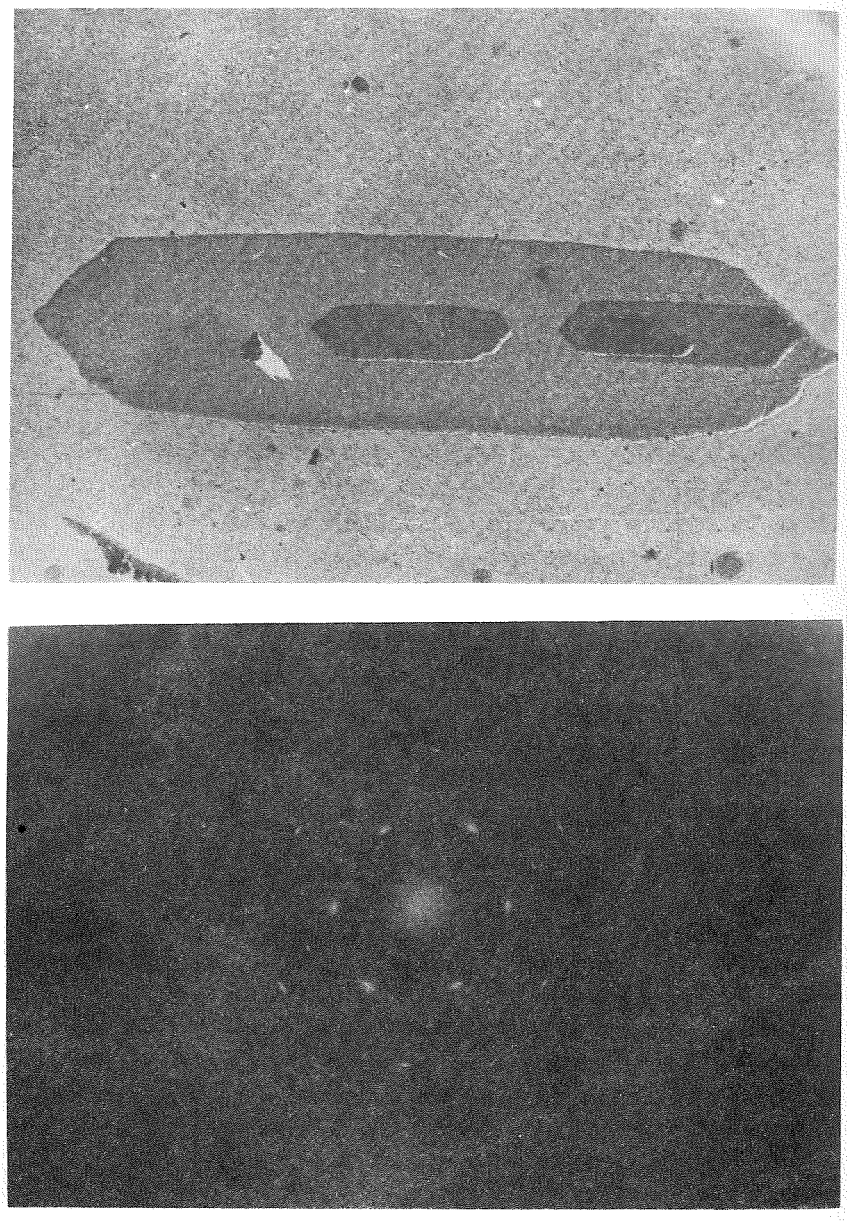

Fig. 14. Monocrystals of poly(styrene-*b*-ϵ-caprolactone) B4 (see Table I) and related electron diffraction pattern.

scattering pattern agree with a close similarity between PCL blocks and the related homopolymer. Indeed, the polyester chains are perpendicular to the surface of lamellae, the crystal is elongated in the direction of the *b* axis of the orthorhombic cell, and the formation of screw dislocations is commonly observed. As a rule, structure formed by monocrystals of copolymer B4 agrees with a model where crystalline lamellae of folded PCL blocks are sandwiched between layers of amorphous PS blocks. A further paper will focus on this remarkable organization of PS–PCL block polymers with a special emphasis on the epitaxial growth of PCL blocks on trioxane.

J. H. is indebted to IRSIA for a fellowship. The authors are grateful to Prof. H. Berghmans and Dr. N. Overbergh (Katholieke Universiteit te Leuven, Belgium) for their helpful collaboration in transmission electron microscopy. Monocrystals were prepared by Dr. J. J. Herman (Solvay Co.) under the guidance of Dr. B. Lotz and Dr. J. C. Wittman (Institut Charles Sadron, CRM, Strasbourg, France); their contribution is greatly appreciated and will be the topic of a forthcoming paper.

References

1. G. E. Molau, in *Block Polymers*, S. L. Aggarwal, Ed., Plenum Press, New York, 1970, p. 79.
2. G. Holden and N. R. Legge, in *Thermoplastic Elastomers: A Comprehensive Review*, N. R. Legge, G. Holden, and H. E. Schroeder, Eds., Hanser Publishers, New York, 1987, Chap. 3.
3. G. Riess, J. Periard, and A. Banderet, in *Colloidal and Morphological Behavior of Block and Graft Copolymers*, G. E. Molau, Ed., Plenum Press, New York, 1971, p. 173.
4. G. Riess, P. Bahadur, and G. Hurtrez, in *Encyclopedia of Polymer Science and Engineering*, 2nd ed., John Wiley & Sons, New York, 1985, Vol. 2, p. 324.
5. G. Maglio and R. Palumbo, in *Polymer Blends, Processing, Morphology and Properties*, M. Kryszewski, A. Galeski, and E. Martuscelli, Eds., Plenum Press, New York, 1983, Vol. 2.
6. R. Fayt, R. Jerome, and Ph. Teyssie, Makromol. Chem., **187**, 837 (1986).
7. M. Schlienger, Ph.D. Thesis, Mulhouse, France, 1976.
8. R. Buscall, T. Corner, and J. F. Stageman, *Polymer Colloids*, Elsevier Applied Publ., 1985.
9. Y. Yamashita and Y. Tsukahara, in *Modification of Polymers*, C. E. Carraher, Jr. and J. A. Moore, Eds., Plenum Press, New York, 1983, p. 131.
10. Union Carbide, Bulletin F 42501 (1969).
11. O. Olabisi, L. E. Robeson, and M. T. Shaw, in *Polymer–Polymer Miscibility*, Academic Press, New York, 1979.
12. C. G. Pitt, M. M. Gratzl, G. L. Kimmel, J. Surles, and A. Schindler, *Biomaterials*, **2**, 215, 1981.
13. Ph. Teyssie, *ACS Symp. Ser.*, **175**, 307 (1981).
14. Ph. Teyssie, J. P. Bioul, A. Hamitou, J. Heuschen, L. Hocks, R. Jerome, and T. Ouhadi, *ACS Symp. Ser.*, **59**, 165 (1977).
15. J. Heuschen, R. Jerome, and Ph. Teyssie, *Macromolecules*, **14**, 242 (1981).
16. J. J. Herman, R. Jerome, Ph. Teyssie, M. Gervais, and B. Gallot, *Makromol. Chem.*, **179**, 1111 (1978).
17. M. Gervais, B. Gallot, R. Jerome, and Ph. Teyssie, *Makromol. Chem.*, **182**, 989 (1981).
18. J. J. Herman, R. Jerome, Ph. Teyssie, M. Gervais, and B. Gallot, *Makromol. Chem.*, **182**, 997 (1981).
19. R. Peret and A. Skoulios, *Makromol. Chem.*, **156**, 157 (1972).
20. J. V. Koleske and R. D. Lundberg, *J. Polym. Sci., A2*, **7**, 795 (1969).
21. C. G. Seefried and J. V. Koleske, *J. Macromol. Sci., Phys.* **B10**, 579 (1974).
22. J. Brandrup and E. R. Immergut, *Polymer Handbook*, Interscience, New York, 1966.
23. J. V. Koleske and R. D. Lundberg, *J. Polym. Sci., A2*, **7**, 897 (1969).
24. L. M. Robeson, *J. Appl. Polym. Sci.*, **17**, 3607 (1973).
25. C. J. Ong, Ph.D. Thesis, University of Massachusetts, Amherst, 1973.
26. B. Gallot, in *Liquid Crystalline Order in Polymers*, A. Blumstein, Ed., Academic Press, New York, 1978, p. 191.

27. L. J. Broutman and B. D. Agarwal, *Polym. Eng. Sci.*, **14**, 581 (1974).
28. B. Wunderlich, *Macromolecular Physics I and II*, Academic Press, New York, 1973.
29. A. J. Kovacs, B. Lotz, and A. Keller, *J. Macromol. Sci. Phys.*, **B3**, 385 (1969).
30. J. C. Wittman, Ph.D. Thesis, CRM Strasbourg, France, 1971.
31. E. Martuscelli, M. Pracella, and M. Pirozzi, *Polymer*, **18**, 887 (1977).
32. P. Cavallo, E. Martuscelli, and M. Pracella, *Polymer*, **18**, 891 (1977).
33. B. Lotz and A. J. Kovacs, *Kolloid-Z.u.Z-Polymere*, **209**, 97 (1966).
34. B. Lotz, A. J. Kovacs, G. A. Bassett, and A. Keller, *Kolloid-Z.u.Z-Polymere*, **209**, 115 (1966).
35. A. J. Kovacs and J. A. Manson, *Kolloid-Z.u.Z-Polymere*, **214**, 1 (1966).
36. D. J. Blundell, A. Keller, and A. J. Kovacs, *J. Polym. Sci.*, **B4**, 481 (1966).

Received February 29, 1988
Accepted July 1, 1988